

# A No-disturbance Startup Scheme for PMSM Speed Loop with Auto-tuned Current Loop

Yihui Cao, Junzheng Wang, Wei Shen

Beijing Institute of Technology, Beijing 100081, P. R. China

E-mail: sw\_she@bit.edu.cn

**Abstract:** Incremental encoder is commonly used for identifying the rotor position of a permanent-magnet synchronous motor (PMSM) in industrial applications. However, initial rotor position error exists when the conventional UVW algorithm is applied, thus uncertain disturbance occurs when Z-pulse correcting. In order to eliminate the preliminary identifying error and obtain the accurate rotor position immediately, a practical and efficient algorithm is proposed. In the proposed initial rotor identifying algorithm, the proper current vector is selected for each sector, and the accurate rotor position can be obtained in a movement of 60 electrical degrees in the worst case. A current loop auto-tuning method based on parameter estimation and frequency domain design is also proposed to construct a no-disturbance startup PMSM servo system for verifying the benefit of the proposed initial rotor identifying algorithm. Finally, comparative experiments between the conventional UVW algorithm and proposed initial rotor identifying algorithm in no-load and load case were conducted in TMS320F28335-based platform, which demonstrates the correctness and effectiveness of the proposed algorithms.

**Key Words:** Initial rotor identifying, Current loop auto-tuning, Parameter estimation, Frequency domain design

## 1 Introduction

PMSM servo system has been widely used in various industrial applications for the past decades. Though having been studied for a long time, high performance, high reliability, and high user-friendliness are being pursued by researchers all the time. In most PMSM servo system, field-oriented control (FOC) scheme with PI cascade strategy has been adopted. It's due to the simplicity and high robustness of PI strategy. Even though this scheme has been applied widely, there is a lot to do to achieve highly reliable and user-friendly control.

One of the significant problems is to obtain accurate rotor position. Currently, rotor position identifying methods can be categorized into two types: sensorless and sensed. In the sensorless case, methods based on back electromotive force(EMF) [1] and high-frequency carrier-signal injection (Rotating Voltage Carrier-Signal Injection and Pulsating Voltage Carrier-Signal Injection typically) [2–4] are usually used to identify the rotor position. However, back-EMF methods can't be applied at low speed or zero speed since the back-EMF is tiny in that time; high-frequency carrier-signal injection methods reveal different weaknesses, such as a deleterious impact on control performance, increasing the system power loss, and so on. In the sensed case, various sensors like resolver, absolute encoder, incremental encoder, are often applied. Among them, the incremental encoder is used most widely because of the cheapness, reliability, and user-friendliness. But the incremental encoder doesn't provide absolute position information without the help of other devices. Thus the commutation signal(or UVW hall signal) is often obtained by hall sensor to identify the initial rotor position in order to supply absolute rotor position information with an incremental encoder, which is called UVW-identifying method.

Nevertheless, in the conventional UVW-identifying method, a 30 electrical degree error at most exists at the

start and it's corrected when Z pulse is encountered, which disrupts the MPTA control from the beginning and causes an unknown disturbance when the motor is starting-up. To solve this problem, methods based on steady-state periodic responses of angle loop [5], phase controlling [6], binary search [7], and other principles [8, 9], were proposed. However, most of these methods were not very practical, and little attention has been focused on the demonstration of the benefit of initial rotor identification in the whole PMSM servo system. To this end, this paper gives a practical initial rotor position identifying algorithm and constructs a no-disturbance startup PMSM control system with an auto-tuned current loop based on it (Fig. 1(a)). Furthermore, two main techniques are considered in this paper: the parameter auto-tuning of the current loop, the initial identifying of absolute rotor position with an incremental encoder.

The outline of the paper is given as follows. Section 1 introduces the research background and the motivation of the work. Section 2 presents the mathematical background of this paper and the auto-tuning of the current loop. Section 3 proposed a new initial rotor position identifying algorithm in no-load and unknown-load case. The effectiveness of the proposed method and algorithm is verified through the experiment in section 4. Finally, remarks and conclusions are made in section 5.

## 2 PMSM Control with Auto-tuned Current Loop

This section gives some mathematical background of the system and discusses auto-tuning the current loop.

### 2.1 PMSM model with inaccurate rotor position

PMSM dynamic model is usually constructed in d-q rotating reference frame, given by [3, 10, 11]:

$$\begin{bmatrix} u_d \\ u_q \end{bmatrix} = \begin{bmatrix} R_s + L_d p & -\omega_r L_q \\ \omega_r L_d & R_s + L_q p \end{bmatrix} \begin{bmatrix} i_d \\ i_q \end{bmatrix} + \begin{bmatrix} 0 \\ \omega_r \psi_r \end{bmatrix} \quad (1)$$

$$T_e = \frac{3}{2} p_n [\psi_r i_q + (L_d - L_q) i_d i_q]. \quad (2)$$

where  $u_d, u_q, i_d, i_q, L_d, L_q$  denote d- and q-axis stator voltage, stator current, stator inductance;  $R_s, \omega_r, \psi_r$  are stator

This work was supported by the National Natural Science Foundation of China under Grant 61873032.

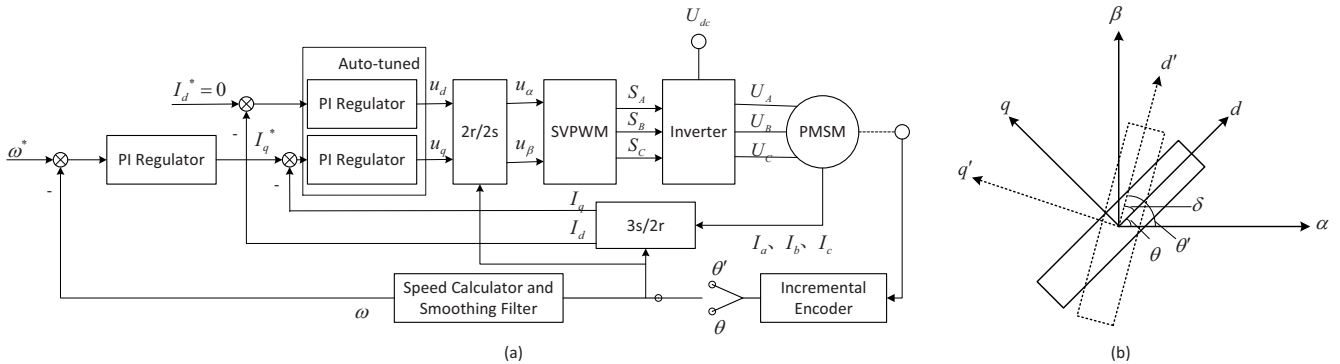


Fig. 1: PMSM control system with auto-tuned current loop: (a) the system diagram; (b) d-q reference frame with accurate and inaccurate rotor position

phase resistance, rotor electrical angular speed, rotor flux;  $T_e, p_n$  are electromagnetic torque, number of pole pairs.  $p$  is differential operator.

When incremental encoder and three hall sensors(or commutation signals) are used to acquire the absolute position information, the rotor position is not accurate initially. Let  $\theta$  denotes the actual rotor position,  $\theta'$  denotes the absolute rotor position obtained from the hall sensors and incremental encoder, and  $\delta = \theta' - \theta$ , as shown in Fig. 1(b). Then the actual d- and q-axis current can be obtained:

$$\begin{bmatrix} i_d \\ i_q \end{bmatrix} = \begin{bmatrix} \cos \delta & -\sin \delta \\ \sin \delta & \cos \delta \end{bmatrix} \begin{bmatrix} i'_d \\ i'_q \end{bmatrix} \quad (3)$$

where  $i'_d, i'_q$  denote the d- and q-axis current acquired from a-, b-, c-axis with transformation in the case of inaccurate rotor position.

Denote the transfer matrix from d'-q' axis to d-q axis as  $T_0 = \begin{bmatrix} \cos \delta & -\sin \delta \\ \sin \delta & \cos \delta \end{bmatrix}$ , then the actual d- and q-axis voltage can be given by:

$$\begin{bmatrix} u_d \\ u_q \end{bmatrix} = T_0 \begin{bmatrix} u'_d \\ u'_q \end{bmatrix} \quad (4)$$

which is similar as equation (3).

By substituting equation (3) and (4) to equation (1), and note that  $T_0^{-1} = \begin{bmatrix} \cos \delta & \sin \delta \\ -\sin \delta & \cos \delta \end{bmatrix}$ , the voltage equation in d'-q' reference frame can be acquired:

$$\begin{aligned} \begin{bmatrix} u'_d \\ u'_q \end{bmatrix} = & \begin{bmatrix} R_s + (L_d \cos^2 \delta + L_q \sin^2 \delta)p + (L_d - L_q)\omega_r \sin \delta \cos \delta \\ -(L_d - L_q) \sin \delta \cos \delta p + \omega_r(L_d \cos^2 \delta + L_q \sin^2 \delta) \\ -(L_d - L_q) \sin \delta \cos \delta p + \omega_r(L_d \sin^2 \delta - L_q \cos^2 \delta) \\ R_s + (L_d \sin^2 \delta + L_q \cos^2 \delta)p - (L_d - L_q)\omega_r \sin \delta \cos \delta \end{bmatrix} \\ & \cdot \begin{bmatrix} i'_d \\ i'_q \end{bmatrix} + \begin{bmatrix} \omega_r \psi_r \sin \delta \\ \omega_r \psi_r \cos \delta \end{bmatrix} \end{aligned} \quad (5)$$

By substituting equation (3) to (2), the initial electromagnetic torque (electromagnetic torque with inaccurate rotor position) can be derived as:

$$T'_e = \frac{3}{2}p \{ \psi_r(i'_d \sin \delta + i'_q \cos \delta) + (L_d - L_q) \left[ \frac{1}{2}(i'^2_d - i'^2_q) \sin 2\delta + i'_d i'_q \cos 2\delta \right] \}. \quad (6)$$

Further, for  $I_d = 0$  control and  $L_d = L_q = L_s$  (consider SPMSM only), the voltage equation in d'-q' reference frame becomes:

$$\begin{bmatrix} u'_d \\ u'_q \end{bmatrix} = \begin{bmatrix} R_s + L_s p & -\omega_r L_s (\sin^2 \delta - \cos^2 \delta) \\ \omega_r L_s & R_s + L_s p \end{bmatrix} \begin{bmatrix} i'_d \\ i'_q \end{bmatrix} + \begin{bmatrix} \omega_r \psi_r \sin \delta \\ \omega_r \psi_r \cos \delta \end{bmatrix} \quad (7)$$

and the initial electromagnetic torque can be written as follows:

$$T'_e = \frac{3}{2}p \psi_r i'_q \cos \delta \quad (8)$$

After that, the PMSM model with inaccurate rotor position (or in d'-q' reference frame) in the system considered is given by the above equations (7) and (8).

## 2.2 Current loop auto-tuning

### 2.2.1 $L_s, R_s$ estimation

In some circumstances, for example, the nameplate of the motor is abraded, or the motor has been used for quite a long time, the machine parameters may be not clear. Hence the electrical parameters should be estimated, which is discussed in this subsection.

From equation (7), when the rotor is locked, i.e.  $\omega_r = 0$ , the relationship of  $u'_q$  and  $i'_q$  is given by:

$$u'_q = (R_s + L_s p)i'_q = i'_q R_s + L_s \frac{d i'_q}{d t} \quad (9)$$

or written in frequency domain as:

$$\frac{I'_q(s)}{U'_q(s)} = \frac{1}{R_s + sL_s} \quad (10)$$

from which the  $I'_q$  current model is linear.

The PMSM parameters  $L_s, R_s$  can be estimated by some linear estimation methods. For simplicity, Linear Regression(LR) were applied in this paper.

Given a reference signal  $u'_q(t) = A_m \sin(\omega t)$ , in the case of rotor locked, the output  $i'_q(t)$  can be denoted by:

$$\begin{aligned} i'_q(t) &= A_f \sin(\omega t + \phi) \\ &= [\sin(\omega t) \quad \cos(\omega t)] \begin{bmatrix} A_f \cos \phi \\ A_f \sin \phi \end{bmatrix} \end{aligned} \quad (11)$$

Denote  $a_1 = A_f \cos \phi$ ,  $a_2 = A_f \sin \phi$ ,  $x_1(t) = \sin(\omega t)$ ,  $x_2(t) = \cos(\omega t)$ ,  $y(t) = i'_q(t)$ , and assume the measurement error  $e(t)$  as white noise, then the output equation becomes:

$$y(t) = [x_1(t) \quad x_2(t)] \begin{bmatrix} a_1 \\ a_2 \end{bmatrix} + e(t) \quad (12)$$

which is the standard form of linear regression.

Next, by sampling the  $I'_q$  model in a step size of  $h$ , i.e. let  $t = 0, h, 2h, \dots, nh$ , and denoting  $\mathbf{Y}^T = [y(0) \quad y(h) \dots y(nh)]$ ,  $\Phi^T = \begin{bmatrix} x_1(0) & x_1(h) & \dots & x_1(nh) \\ x_2(0) & x_2(h) & \dots & x_2(nh) \end{bmatrix}$ , the least square estimation of  $a_1, a_2$  can be given by:

$$\begin{bmatrix} a_1^* \\ a_2^* \end{bmatrix} = (\Phi^T \Phi)^{-1} \Phi^T \mathbf{Y} \quad (13)$$

Then the origin parameters  $L_s, R_s$  can be obtained from the equation of the amplitude ratio and phase difference:

$$\begin{aligned} \frac{A_f}{A_m} &= \frac{\sqrt{a_1^{*2} + a_2^{*2}}}{A_m} = \frac{1}{\sqrt{R_s^2 + (\omega L_s)^2}} \\ \tan \phi &= \frac{a_2^*}{a_1^*} = \frac{\omega L_s}{R_s} \end{aligned} \quad (14)$$

## 2.2.2 Loop auto-tuning

Once parameters  $L_s, R_s$  were estimated well, the current loop can be auto-tuned [11, 12]. Fig. 2 shows the simplified current loop diagram, in which q-axis current  $I_q$  and voltage  $U_q$  are used in per unit(divided by  $U_{base}$  and  $I_{base}$ );  $K_p^i, K_i^i$  denote the PI control parameters;  $T_{PWM}$  describes the equivalent time constant of IPM module;  $T_{cf}$  indicates the filter constant; and the gain  $K_{PWM} = \frac{U_{dc}/\sqrt{3}}{I_{base}}$ , back-EMF  $\tilde{e} = \frac{e}{I_{base}}$ .

The open-loop transfer function of the system can be given by:

$$\begin{aligned} G_{oi}(s) &= K_p^i \left(1 + \frac{K_i^i}{s}\right) \cdot \frac{K_{PWM}}{T_{PWM}s + 1} \cdot \frac{1}{L_s s + R_s} \cdot \frac{1}{T_{cf}s + 1} \\ &= \frac{K \left(\frac{1}{K_i^i} s + 1\right)}{s \left(\frac{L_s}{R_s} s + 1\right) (T_{cf}s + 1) (T_{PWM}s + 1)} \end{aligned} \quad (15)$$

where  $K = \frac{K_p^i K_i^i K_{PWM}}{R_s}$ .

Typically, the inequality  $T_{cf}, T_{PWM} \ll \frac{L_s}{R_s}$  holds, thus the relevant two lag components can be simplified to one lag component, which has a time constant  $T_{ck} = T_{cf} + T_{PWM}$ . To this end, the system given by equation (15) can be further simplified to a 3-order one, given by:

$$G_{oi}(s) = \frac{K \left(\frac{1}{K_i^i} s + 1\right)}{s \left(\frac{L_s}{R_s} s + 1\right) (T_{ck}s + 1)} \quad (16)$$

From the approximate amplitude frequency characteristic of above open-loop transfer function (Fig. 3), the current loop can acquire both high bandwidth and high stability easily if  $\frac{1}{T_{ck}}$  is large enough.

Choose the integral gain  $K_i^i$  as  $K_i^i = \frac{R_s}{L_s}$ , then the proportional gain  $K_p^i$  can be obtained when the desired current

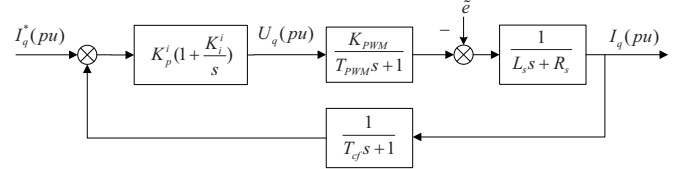


Fig. 2: Simplified current loop diagram

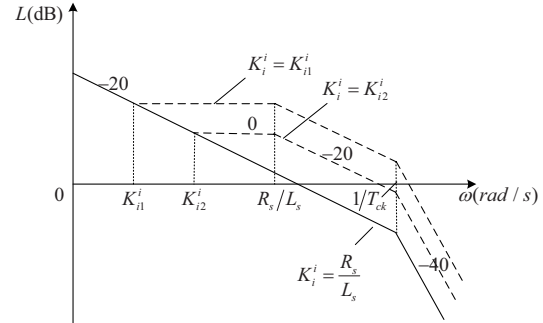


Fig. 3: Approximate open-loop amplitude frequency response characteristic

loop bandwidth is given. Assuming the desired current loop bandwidth is  $\omega_{cs}$ , then the following equation holds:

$$|G_{oi}(j\omega_{cs})| = \left| \frac{K_p^i K_{PWM} / L_s}{j\omega_{cs} (j\omega_{cs} T_{ck} + 1)} \right| = 1 \quad (17)$$

which gives  $K_p^i = \frac{L_s \omega_{cs}}{K_{PWM}} \sqrt{(\omega_{cs} T_{ck})^2 + 1}$ .

That is, the current loop control parameters can be auto-tuned by:

$$\begin{aligned} K_p^i &= \frac{L_s \omega_{cs}}{K_{PWM}} \sqrt{(\omega_{cs} T_{ck})^2 + 1} \\ K_i^i &= \frac{R_s}{L_s} \end{aligned} \quad (18)$$

## 3 Proposed Low-cost Pre-positioning Algorithm

In order to start up the PMSM with no-disturbance, a low-cost pre-positioning algorithm based on positioning current vector selecting is proposed. This algorithm considers two circumstances: with no load and with unknown load, which is explained in the following.

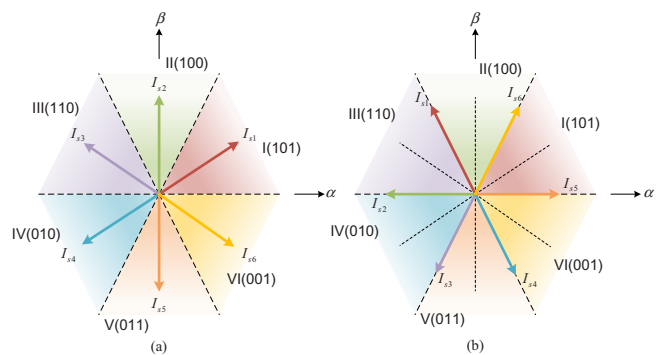


Fig. 4: Current positioning vector selection map in various sectors

### 3.1 With no load

The initial mechanical equation of the PMSM motor can be given as:

$$T'_e - T_l = (J_m + J_l) \frac{d\omega_r}{dt} \quad (19)$$

where  $T_l$  is the load torque;  $J_m$  is the moment of inertia of the motor,  $J_l$  is the equivalent moment of inertia of the load.

When there is no load ( $T_l = 0, J_l = 0$ ), from equation (19), the PMSM motor can attain high angular acceleration with low electromagnetic torque which leads to motor moving for correcting rotor position. Therefore a method with low torque but high efficiency is explained as follows.

As shown in Fig. 4(a), the commutation signal divides the still stator  $\alpha - \beta$  plane into six sectors. For each sector, when the rotor is located here, a corresponding current vector is chosen to pre-position the rotor (Table 1). It's obvious that the motor will move to the center of the sector immediately, and it takes no more than  $30^\circ$  in electrical angle during the whole correcting process (almost not move).

Table 1: Pre-positioning Current Vector Chosen in Different Cases

Sector name (vector)	No-load case ( $I_d + jI_q$ )	Unknown-load case ( $I_d + jI_q$ )
I ( $I_{s1}$ )	$I_{smax}(\frac{\sqrt{3}}{2} + j\frac{1}{2})$	$I_{smax}(-\frac{1}{2} + j\frac{\sqrt{3}}{2})$
II ( $I_{s2}$ )	$I_{smax} \cdot j1$	$-I_{smax}$
III ( $I_{s3}$ )	$I_{smax}(-\frac{\sqrt{3}}{2} + j\frac{1}{2})$	$I_{smax}(-\frac{1}{2} - j\frac{\sqrt{3}}{2})$
IV ( $I_{s4}$ )	$I_{smax}(-\frac{\sqrt{3}}{2} - j\frac{1}{2})$	$I_{smax}(\frac{1}{2} - j\frac{\sqrt{3}}{2})$
V ( $I_{s5}$ )	$-I_{smax} \cdot j1$	$I_{smax}$
VI ( $I_{s6}$ )	$I_{smax}(\frac{\sqrt{3}}{2} - j\frac{1}{2})$	$I_{smax}(\frac{1}{2} + j\frac{\sqrt{3}}{2})$

### 3.2 With unknown load

When it comes to unknown load ( $T_l \neq 0$ , or  $J_l \neq 0$ ), from equation (19), if the electromagnetic torque is low, the motor's acceleration will be too tiny to overcome the friction and start up the motor. To this end, the revised method is proposed to solve the problem, yet some cost is added.

The revised method is based on the detection of the change of the commutation signal. In the still stator  $\alpha - \beta$  plane, each sector corresponds to one value of commutation signal (Fig. 4(b)). For each sector, the current vector orthogonal to the central vector in the counterclockwise direction is selected as pre-positioning current vector (Table 1). When the pre-positioning current vector is implemented, the motor will move. Once the commutation signal changes, which indicates the rotor is moving from one sector to another, the actual rotor position will be obtained, and then the pre-positioning process ends. In this method, the motor will move no more than  $60^\circ$  in electrical angle during the whole correcting process. Moreover, from equation (8), the initial electromagnetic torque with inaccurate rotor position is no less than 0.866 time of maximum electromagnetic torque (i.e.  $T'_e \geq 0.866T_e$ ). Hence the initial rotor position can be identified when most of the load is being applied.

### 3.3 Low-cost pre-positioning algorithm

According to the above two subsections, the low-cost pre-positioning algorithm for motor no-disturbance startup scheme is described as follows (Fig. 5):

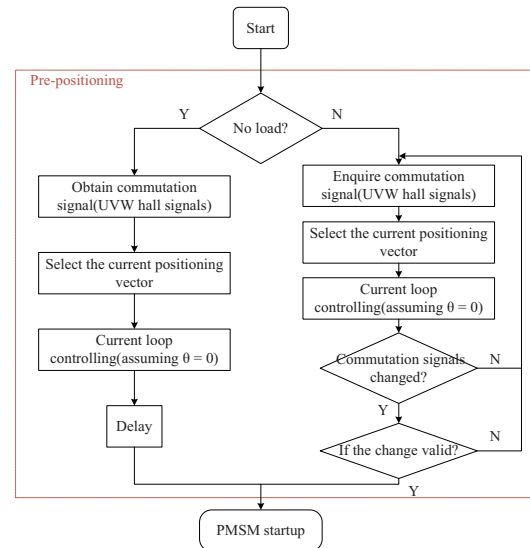


Fig. 5: Proposed low-cost pre-positioning algorithm

- 1) The algorithm starts with judging if there is load ( $T_l, J_l$ ) manually.
- 2) For both situation (no-load and unknown-load cases), current positioning vector is chosen for different initial rotor position first. Afterwards the current loop is controlled to implement the current positioning vector. Note that the current loop is implemented in  $\alpha - \beta$  reference frame (i.e. assuming the transformation angle  $\theta \equiv 0$ ), and similar control effect as in d-q reference frame can be acquired, in that the disturb back-EMF is small during the pre-positioning.
- 3) Note that the amplitude of current positioning vector needs a little trial-and-error.

### 4 Proposed Algorithms to No-disturbance Startup Scheme

With the auto-tuning method of the current loop and the proposed low-cost pre-positioning algorithm given above, a no-disturbance startup scheme has been constructed. To validate the proposed method/algorithm, relevant experiments were conducted in the hardware platform shown in Fig. 6. The platform consists of a main AC drive circuit, a loading system, and an experimental electrical machine. In the main AC drive circuit, a TMS320F28335 DSP executes the PI-cascade control program and the proposed no-disturbance startup algorithm; a 3-phase voltage source inverter works at a switching frequency of 10kHz and the data sampling frequency is 1kHz. The machine parameters of the experimental motor are summarized in Table 2.

Table 2: Parameters of Experimental SPMSM

Parameter	Nominal Value
Rated Power $P_N$	750W
Rated Torque $T_N$	2.39 N · m
Rated Speed $n_{nom}$	3000rpm
Rotor Inertia $J_m$	1.03 kg · cm <sup>2</sup>
Torque Coefficient $K_t$	0.4 N · m/A
Pole Pair $p_n$	4
Stator Resistor $R_s$	1.6Ω
Stator Inductance $L_s$	4.0mH

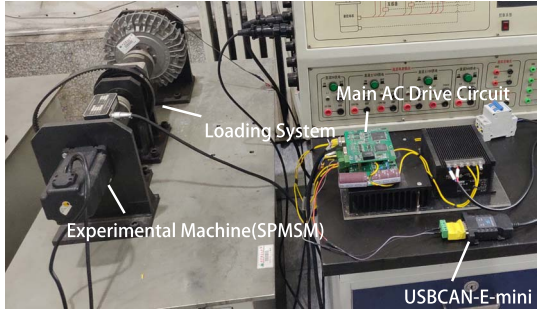


Fig. 6: Experimental hardware platform

#### 4.1 $L_s$ , $R_s$ estimation and current loop auto-tuning

In order to construct the auto-tuned current loop first, the experimental estimation of the machine parameters  $L_s$ ,  $R_s$  was conducted in advance. As described in Section 2.2.1, the rotor of SPMSM was locked mechanically beforehand to ensure  $\omega_r = 0$ . Next sinusoidal q'-axis voltages  $v'_q$  of several different frequencies were applied in the experimental machine respectively, and the corresponding q'-axis currents were acquired.

The parameters  $a_1, a_2$  can be calculated from equation (13). And ideally, the estimation results of the origin parameters  $L_s, R_s$  can be then derived from equation (14). However, in reality, the waveform of the actual q'-axis current response was distorted mainly because of the deadtime of PWM signals. Nevertheless, the phase difference can be well-estimated. Therefore  $\frac{R_s}{L_s}$  can be estimated (Table 3).

Table 3: Parameters Estimated from Nominal Stator Resistor( $R_s = 1.6\Omega$ ) and  $I'_q$  Current Excitation

Frequency $\omega$ (Hz)	Estimated $\frac{R_s}{L_s}$	Estimated Stator Inductance $L_s$ (H)
10	373.3	0.0043
20	463.9	0.0034
25	482.5	0.0033

Take the average value of the estimated values in Table 3 as the final estimated parameters, then  $\hat{R}_s = 1.6\Omega$ ,  $\hat{L}_s = 0.0037H$ . Substitute the estimation results to equation (18), and note that  $K_{PWM} = 18.19$  and take the desired cut-off frequency of speed loop  $\omega_{cs}$  as  $6280rad/s$ , then the auto-tuned current loop control parameters can be given by:

$$K_p^i = \frac{\hat{L}_s \omega_{cs}}{K_{PWM}} \sqrt{(\omega_{cs} T_{ck})^2 + 1} \approx 1.27 \quad (20)$$

$$K_i^i = \frac{\hat{R}_s}{\hat{L}_s} = 432$$

#### 4.2 Proposed algorithms to no-disturbance startup scheme

To verify the proposed low-cost pre-positioning algorithm for initial rotor identification and demonstrate the benefit of it in the complete PMSM servo system, a startup experiment was designed based on the constructed auto-tuned current loop, and both no-load and unknown-load experiments were conducted.

No-load experiments were carried on as follows: firstly, set the software switch flag  $lsw = 0$  to enter the pre-

positioning mode once the machine is powered up; then revise the flag  $lsw = 1$  manually to enter the speed control mode(given a constant speed 450rpm). The results are depicted in Fig. 7 and Fig. 8. Among them, the subgraph 1 denotes the speed curve during the whole startup process; the subgraph 2 and 3 denotes the speed change at the moment when  $lsw = 0$  and  $lsw = 1$  respectively; the subgraph 4 and 5 denotes the  $I_a, I_b$  curves in the moment when  $lsw = 0$  and  $lsw = 1$  respectively.

In the no-load startup process when the conventional algorithm was executed (Fig. 7), the machine was powered up normally at about 2s, the speed stepping happened at 4.1s, and a mutation in speed took place at 4.2s or so. The mutation in speed is due to the correcting of rotor position when Z pulse is encountered, and it brings uncertain disturbance to the digital control. To be more detailed, the inaccurate initial rotor position not only makes it impossible to start up the machine with MTPA control, but also brings some uncertain disturbance to the system. By comparison, Fig. 8 shows the no-load startup process when the proposed algorithm was executed. In the process (Fig. 8), the machine was pre-positioning at about 2s by proposed algorithm, and then started up with no-disturbance at about 5.2s, which validated the effectiveness of the proposed algorithm in the complete PMSM control system.

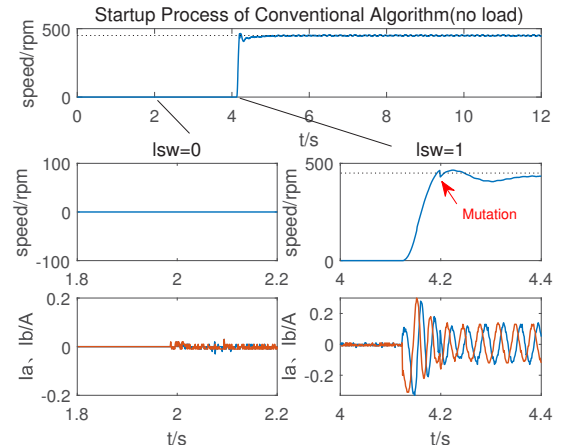


Fig. 7: Startup process of conventional algorithm(no load)

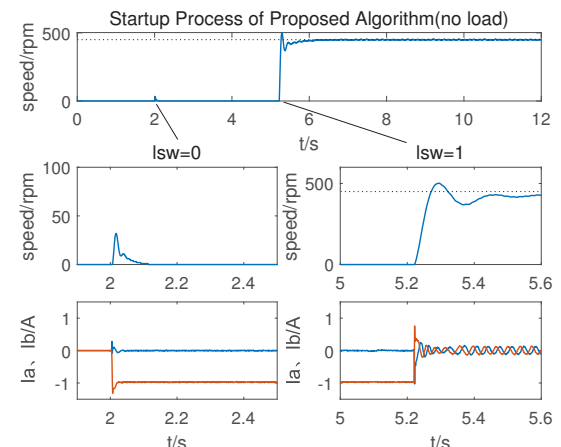


Fig. 8: Startup process of proposed algorithm(no load)

Unknown-load experiments were then implemented by

similar means. In the unknown-load startup process when the conventional algorithm was executed (Fig. 9), the machine was powered up normally at about 2s, the speed stepping happened at 6.2s, and a mutation in speed took place at 6.5s or so. Similarly, the mutation in speed implies that the inaccurate initial rotor position no only makes it impossible to start up the machine with MTPA control but also brings some uncertain disturbance to the system. Fig. 10 denotes the no-load startup process when the proposed algorithm was executed. In the process (Fig. 10), the machine was pre-positioning at about 2s by proposed algorithm, and then start up with no-disturbance at about 11s, which validated the effectiveness of the proposed algorithm in the complete PMSM control system with a load. Note that before the experiments when the proposed algorithm was executed, some trial-and-error were conducted to acquire suitable  $I_{smax}$ .

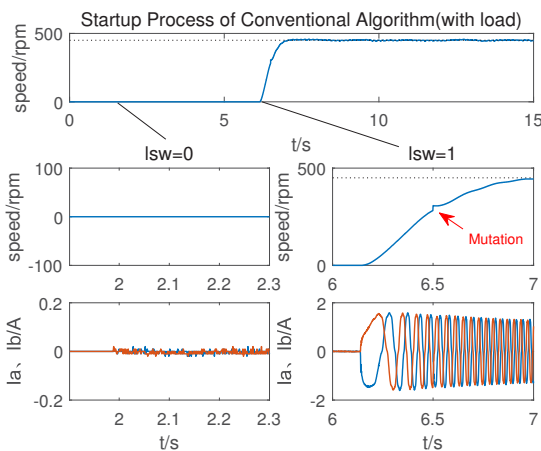


Fig. 9: Startup process of conventional algorithm(with load)

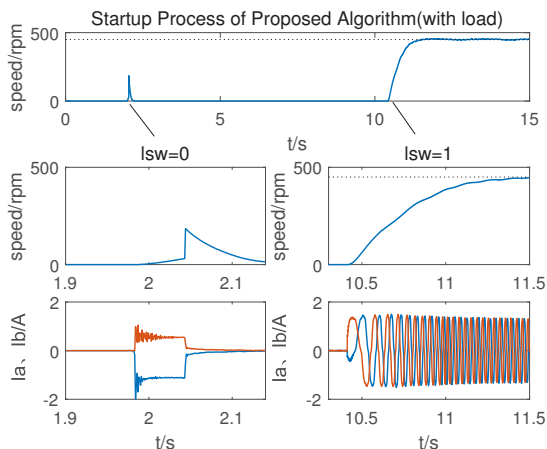


Fig. 10: Startup process of proposed algorithm(with load)

After the experiments above, the no-disturbance startup scheme were demonstrated finally. And thus the proposed method and algorithm were also proved.

## 5 Conclusion

In industrial applications, an incremental encoder is usually used for identifying the rotor position of a PMSM. However, initial rotor position error exists when the conventional UVW algorithm is applied. In this paper, a practical and effi-

cient algorithm for correcting the initial identifying error immediately is proposed, and a PMSM control system with an auto-tuned current loop is constructed to demonstrate the effectiveness of the algorithm. For the no-load case, a central current vector is selected to pre-position the rotor for each sector; for the unknown-load case, an almost-orthogonal sector is selected to move the rotor for pre-positioning in each sector. Both of them are supported by an auto-tuned current loop, which is based on the LS estimation of motor parameters and the frequency domain design. Finally, comparative experiments were conducted in a TMS320F28335-based hardware platform, and the results proved the correctness and effectiveness of the proposed algorithm and relevant method. High performance and auto-tuning of the speed loop will be studied in the constructed no-disturbance startup system in the future.

## References

- [1] Z. Wang and Y. Ye, "Research on self-startup states process of back-emf based sensorless vector control of pmsm," *Electric Machines and Control*, vol. 15, no. 10, pp. 36–42, 2011.
- [2] H. Kim, K.-K. Huh, R. D. Lorenz, and T. M. Jahns, "A novel method for initial rotor position estimation for ipm synchronous machine drives," *IEEE Transactions on Industry Applications*, vol. 40, no. 5, pp. 1369–1378, 2004.
- [3] J.-S. Kim and S.-K. Sul, "New approach for high-performance pmsm drives without rotational position sensors," *IEEE Transactions on Power Electronics*, vol. 12, no. 5, pp. 904–911, 1997.
- [4] H. Li, X. Zhang, S. Yang, and E. Li, "Review on sensorless control of permanent magnet synchronous motor based on high-frequency signal injection," *Transactions of China electronical society*, vol. 33, no. 12, pp. 2653–2664, 2018.
- [5] D.-H. Jung and I.-J. Ha, "An efficient method for identifying the initial position of a pmsm with an incremental encoder," *IEEE Transactions on Industrial electronics*, vol. 45, no. 4, pp. 682–685, 1998.
- [6] J. Zhang and N. Wu, "Identification of initial rotor position of a micro-pmsm," in *2008 10th International Conference on Control, Automation, Robotics and Vision*, pp. 476–481. IEEE, 2008.
- [7] F. Teng, Y. Hu, and W. Huang, "Amending algorithm to measure motors initial position in pmsm servo systems," *Proceedings of the CSEE*, vol. 28, no. 27, pp. 109–113, 2008.
- [8] R. Hu, "Initial rotor position estimation for pmsm," Ph.D. dissertation, Harbin Institute of Technology, 2008.
- [9] X. Kang, S. Wang, J. Lu, X. Hui, and W. Guoqiang, "A method of initial orientation for pmsm," *Electric Drive Automation*, vol. 35, no. 5, pp. 20–23, 2013.
- [10] J. Ren, Y. Ye, G. Xu, Q. Zhao, and M. Zhu, "Uncertainty-and-disturbance-estimator-based current control scheme for pmsm drives with a simple parameter tuning algorithm," *IEEE Transactions on Power Electronics*, vol. 32, no. 7, pp. 5712–5722, 2017.
- [11] S.-M. Yang and K.-W. Lin, "Automatic control loop tuning for permanent-magnet ac servo motor drives," *IEEE Transactions on Industrial Electronics*, vol. 63, no. 3, pp. 1499–1506, 2016.
- [12] L. Harnefors and H.-P. Nee, "Model-based current control of ac machines using the internal model control method," *IEEE Transactions on Industry Applications*, vol. 34, no. 1, pp. 133–141, 1998.